

Dynamics of systems with isotropic competing interactions in an external field: a Langevin approach

R. Díaz-Méndez^{1,2,a}, A. Mendoza-Coto^{3,2}, R. Mulet^{3,2}, L. Nicolao⁴, and D.A. Stariolo⁵

¹ Nanophysics Group, Department of Physics, Electric Engineering Faculty, CUJAE, Ave 114 final, La Habana, Cuba

² “Henri-Poincaré-Group” of Complex Systems, Physics Faculty, University of Havana, La Habana, CP 10400, Cuba

³ Department of Theoretical Physics, Physics Faculty, University of Havana, La Habana, CP 10400, Cuba

⁴ Dipartimento di Fisica, Università di Roma “La Sapienza”, P.le Aldo Moro 2, 00185 Roma, Italy

⁵ Departamento de Física, Universidade Federal do Rio Grande do Sul and National Institute of Science and Technology for Complex Systems CP 15051, 91501-970, Porto Alegre, Brasil

Received 10 March 2011

Published online 7 June 2011 – © EDP Sciences, Società Italiana di Fisica, Springer-Verlag 2011

Abstract. We study the Langevin dynamics of a ferromagnetic Ginzburg-Landau Hamiltonian with a competing long-range repulsive term in the presence of an external magnetic field. The model is analytically solved within the self consistent Hartree approximation for two different initial conditions: disordered or *zero field cooled* (ZFC), and fully magnetized or *field cooled* (FC). To test the predictions of the approximation we develop a suitable numerical scheme to ensure the isotropic nature of the interactions. Both the analytical approach and the numerical simulations of two-dimensional finite systems confirm a simple aging scenario at zero temperature and zero field. At zero temperature a critical field h_c is found below which the initial conditions are relevant for the long time dynamics of the system. For $h < h_c$ a logarithmic growth of modulated domains is found in the numerical simulations but this behavior is not captured by the analytical approach which predicts a $t^{1/2}$ growth law at $T = 0$.

1 Introduction

It is now well understood that modulated structures can arise from underlying competing interactions acting upon different scales [1]. In magnetic systems, e.g. in ultrathin magnetic films with perpendicular anisotropy [2,3], these phases are present due to an exchange (ferromagnetic) short range interaction competing with a weaker but long range (antiferromagnetic) dipolar interaction. This competition gives rise to striped and bubbled patterns that break the translational and/or rotational symmetry of the system.

This phenomenology is shared with a large number of systems. Type-II superconductors [4], doped Mott insulators [5], quantum Hall systems [6] and diblock copolymers [7,8] are other examples of systems with competing interactions which have symmetry breaking transitions to inhomogeneous phases. Since domains in these systems often are of mesoscopic scales, it is possible to perform a general analysis which neglects the microscopic details of each specific system while capturing its general properties. A pioneering attempt in this direction was done by Brazovskii [9], who showed that systems in which the spectrum of fluctuations attain a minimum in a shell at a

non-zero wave vector, undergo a first order phase transition to a modulated state driven by fluctuations, in contrast to the second order transition predicted by the mean field theory. Moreover, the presence of competing interactions frequently lead to a proliferation of metastable states at low temperatures that may dominate the dynamical behavior of the system. For the three dimensional case, recent experimental results in colloidal systems [10] report the presence of glassy states, in agreement with theoretical predictions for a model with screened electrostatic repulsion [11] and for a Coulomb frustrated ferromagnet [12–14].

However, it is still far from clear which are the relevant aspects that control the long time dynamics of these systems and, more generally, what kind of dynamics should one expect. In an early work for a model with ferromagnetic and dipolar interactions, Roland and Desai [15] studied the dynamics in the short-time regime, showing that the order parameter evolves to modulated structures. Almost contemporaneously, Elder and Grant [16] obtained a scaling relation for the dynamics of phase ordering of the modulated phases, characterized by a growth law $L \propto t^{1/z}$ with a dynamical exponent $z = 2$. After that, many works were devoted to verify such scaling relation, solving numerically the dynamics of the Swift-Hohenberg

^a e-mail: rogelio@electronica.cujae.edu.cu

model [17,18]. Indeed most of these numerical simulations [19–23] report a late-time regime that satisfies scaling, but with a growth exponent near $z = 5$ for zero temperature quenches and $z = 4$ for low finite temperatures, obtained mainly monitoring the structure factor and related quantities. In [24] an exponent $z = 3$ was observed in zero temperature quenches which was associated to grain boundary motion. For quenches at zero temperature, a dynamic crossover to a frozen state was reported [25], and associated with grain boundary pinning [26]. On the other hand, recent experiments in diblock copolymers [27] (that are assumed to be good model systems for studying phase ordering of modulated structures), show that the late time dynamics of the stripe ordering satisfies scaling with $z = 4$, driven mainly by the annihilation involving tripoles and quadrupoles of disclinations. For a bubble forming system Harrison et al. [28] found the same growth law, but this time dominated by the collapse of smaller grains which reside on the boundary of two larger grains. More recently, Gomez et al. [29] found a logarithmic growth $L(t) \simeq \ln t$ of domains in simulations of an hexagonal diblock copolymer model. The logarithmic growth is attributed to the Lifshitz mechanism of pinning of triple points at grain boundaries. Here we report logarithmic growth of different characteristic length scales in simulations of a stripe forming system. Also, Gleiser et al. [30] found a crossover between an apparently logarithmic relaxation to a $t^{1/2}$ law in the coarsening dynamics of a dipolar frustrated Ising model. So, despite a lot of numerical and experimental effort the question of dynamical universality of modulated systems remains elusive.

Recently, Mulet and Stariolo [31] solved the long time Langevin dynamics of a model with competing interactions in the Hartree (self-consistent field) approximation. For the case of zero external field they showed that the dynamics can be separated in two times scales. In the first one modulated structures emerge, and the behavior resembles the formation of typical ferromagnetic domains [32]. Once these modulated structures are formed the dynamics changes qualitatively, becoming independent of the system dimension and the temperature is a relevant variable. For $T > 0$ the system exhibits interrupted aging and a standard paramagnetic (exponential) relaxation for large times. At low temperatures domains of stripes of finite size, characterized by a finite correlation length, are formed. At $T = 0$ the correlation length diverges and stripes order sets in with a growth law $L \propto t^{1/2}$. Our simulations show that these results are correct in the time scale while the very slow dynamics of topological defects does not play a significant role.

In this work we extend the results of [31] by solving, within the Hartree approximation, the same model in the presence of an external magnetic field and for two different initial conditions. The initial conditions were chosen to mimic standard experimental protocols: in the *zero field cooling* (ZFC) experiment, the system is initialized in a highly disordered state (high temperature and zero external field). After some waiting time the temperature is suddenly lowered towards the modulated phase and the field is

turned on. In the *field cooling* (FC) protocol, the sample is first fully magnetized in the presence of an external field, and then the temperature is decreased keeping the field on. To check the validity of our approximations, we develop a reliable numerical scheme to reach the asymptotic dynamical behavior, while ensuring the isotropic nature of the model interactions. We compare the analytical results with extensive numerical simulations of a two-dimensional magnetic system with dipolar interactions.

The rest of the paper is organized as follows. In Section 2 we present the model and the Hartree approximation to solve its dynamics. We present analytical results for the autocorrelations and spatial correlation functions for zero temperature ($T = 0$) and finite external field (H). Section 3 is devoted to the numerical simulations. It begins with an analysis of the fluctuation spectrum of the model, which is essential to compare the simulations of finite systems and the analytical results. Then we present the numerical scheme used and compare the simulations with the analytical predictions. Finally in Section 4 we summarize and present the conclusions of our work. The details of the calculations are left for the appendices.

2 Analytical approach

We consider an effective Ginzburg-Landau Hamiltonian:

$$\begin{aligned} \mathcal{H}[\phi] = & \int d^d x \left[\frac{1}{2} (\nabla \phi(\mathbf{x}))^2 + \frac{r}{2} \phi^2(\mathbf{x}) \right. \\ & \left. + \frac{u}{4} \phi^4(\mathbf{x}) - h(\mathbf{x}) \phi(\mathbf{x}) \right] \\ & + \frac{1}{2\delta} \int d^d x d^d x' \phi(\mathbf{x}) J(\mathbf{x}, \mathbf{x}') \phi(\mathbf{x}') \end{aligned} \quad (1)$$

where $r < 0$, $u > 0$ and $J(\mathbf{x}, \mathbf{x}') = J(|\mathbf{x} - \mathbf{x}'|)$ represents a repulsive, isotropic, competing interaction. $h(\mathbf{x})$ is an external field and the parameter δ measures the relative intensity between the attractive and repulsive parts of the Hamiltonian. In the limit $\delta \rightarrow \infty$ one recovers the ferromagnetic $O(N)$ model (for $N = 1$) [32–34].

A natural choice for the dynamics of the phenomenological coarse-grained Hamiltonian (1) is the Langevin dynamics:

$$\frac{\partial \phi(\mathbf{x})}{\partial t} = -\Gamma \frac{\delta H[\phi]}{\delta \phi(\mathbf{x})} + \eta(\mathbf{x}, t), \quad (2)$$

which is a phenomenological dynamical equation that describes the relaxation towards thermal equilibrium. It is a purely dissipative dynamics because we are interested in the case of a non-conservative scalar-field order parameter. This equation takes the form:

$$\begin{aligned} \frac{1}{\Gamma} \frac{\partial \phi(\mathbf{x}, t)}{\partial t} = & \nabla^2 \phi(\mathbf{x}, t) - r \phi(\mathbf{x}, t) - u \phi^3(\mathbf{x}, t) + h(\mathbf{x}, t) \\ & - \frac{1}{\delta} \int d^d x' J(\mathbf{x}, \mathbf{x}') \phi(\mathbf{x}', t) + \frac{1}{\Gamma} \eta(\mathbf{x}, t), \end{aligned} \quad (3)$$

where Γ is the mobility coefficient and $\eta(\mathbf{x}, t)$ represents a Gaussian noise that models the coupling to a heat bath.

Within the self-consistent (Hartree) approximation the non-linear term ϕ^3 is substituted by $3\langle\phi^2(\mathbf{x}, t)\rangle\phi(\mathbf{x}, t)$ where the average is performed over the initial conditions and noise realizations. It is worth to note that, within the approximation, $\langle\phi^2(\mathbf{x}, t)\rangle$ is spatially homogeneous, which implies a restriction in the possible ensembles of initial conditions taken to perform the averages.

We have studied two kinds of initial conditions: disordered (zero field cooled) and ferromagnetic (field cooled). Both can be written in the general form

$$\begin{aligned}\langle\phi(\mathbf{x}, 0)\rangle &= \phi_0 \\ \langle\phi(\mathbf{x}, 0)\phi(\mathbf{x}', 0)\rangle &= v(\mathbf{x} - \mathbf{x}').\end{aligned}\quad (4)$$

In this way, the disordered condition ($h = 0$ and $T \gg 0$) is obtained with $\phi_0 = 0$ and $v(\mathbf{x} - \mathbf{x}') = \Delta\delta(\mathbf{x} - \mathbf{x}')$, while the ferromagnetic initial condition ($h \gg 0$) is represented by $\phi_0 > 0$ and $v(\mathbf{x} - \mathbf{x}') = \phi_0^2$.

After applying Fourier transforms, the equation of motion (3) in the Hartree approximation reads:

$$\frac{\partial\hat{\phi}(\mathbf{k}, t)}{\partial t} = -[A(k) + I(t)]\hat{\phi}(\mathbf{k}, t) + \hat{\eta}(\mathbf{k}, t) + \hat{h}(\mathbf{k}, t), \quad (5)$$

with

$$I(t) = r_0 + g\langle\phi^2(\mathbf{x}, t)\rangle, \quad (6)$$

$$A(k) = k^2 + \frac{1}{\delta}\hat{J}(k) - a_0, \quad (7)$$

where $g = 3u$, $a_0 = k_0^2 + 1/\delta\hat{J}(k_0)$ and $r_0 = r + a_0$. k_0 is the wave vector minimizing the spectrum of fluctuations $A(k)$. In the case of isotropic competing interactions it is well established that this quantity has a minimum on a spherical shell of radius k_0 in reciprocal space [9]. Thus, definitions (6) and (7) ensure that $A(k_0) = 0$.

The general solution of the dynamical equations (5) can be written as:

$$\begin{aligned}\hat{\phi}(\mathbf{k}, t) &= \hat{\phi}(\mathbf{k}, 0)R(\mathbf{k}, t, 0) + \int_0^t R(\mathbf{k}, t, t')\hat{\eta}(\mathbf{k}, t')dt' \\ &+ \int_0^t R(\mathbf{k}, t, t')\hat{h}(\mathbf{k}, t')dt'\end{aligned}$$

where $R(\mathbf{k}, t, t') = \frac{Y(t')}{Y(t)}e^{-A(k)(t-t')}$ is the response function and $Y(t) = e^{\int_0^t dt' I(t')}$. The Gaussian thermal noise $\eta(\mathbf{x}, t)$ satisfies

$$\begin{aligned}\langle\hat{\eta}(\mathbf{k}, t)\rangle &= 0, \\ \langle\hat{\eta}(\mathbf{k}, t)\hat{\eta}(\mathbf{k}', t')\rangle &= 2\Gamma T(2\pi)^d\delta(\mathbf{k} + \mathbf{k}')\delta(t - t').\end{aligned}\quad (8)$$

Throughout the rest of the calculations Γ will be set to 1. This is equivalent to transform time as $t \rightarrow t\Gamma$ in equations (8) and (2), so that time is a dimensionless variable. A stationary homogeneous external field ($h(\mathbf{x}, t) = h$) is defined by:

$$\begin{aligned}\langle\hat{h}(\mathbf{k})\rangle &= h(2\pi)^d\delta(\mathbf{k}), \\ \langle\hat{h}(\mathbf{k})\hat{h}(\mathbf{k}')\rangle &= h^2(2\pi)^{2d}\delta(\mathbf{k})\delta(\mathbf{k}').\end{aligned}\quad (9)$$

A complete solution amounts to the determination of the response function, or equivalently, $Y(t)$. Defining $K(t) = Y^2(t)$ and following standard procedures [31], it is possible to reduce the problem to the solution of the following differential equation:

$$\begin{aligned}\frac{dK(t)}{dt} &= 2r_0K(t) + 2gV(t) \\ &+ 4gT\int_0^t d\tau K(\tau)f(t - \tau) \\ &+ 4ghK(t)^{1/2}\phi_0e^{-A(0)t} \\ &\times\int_0^t d\tau K(\tau)^{1/2}e^{-A(0)(t-\tau)} \\ &+ 2gh^2\left[\int_0^t d\tau K(\tau)^{1/2}e^{-A(0)(t-\tau)}\right]^2\end{aligned}\quad (10)$$

where

$$V(t) = \frac{1}{(2\pi)^d}\int d^dk e^{-2A(k)t}\hat{v}(\mathbf{k}) \quad (11)$$

and

$$f(t) = \frac{1}{(2\pi)^d}\int d^dk e^{-2A(k)t}. \quad (12)$$

$V(t)$ contains the information about the initial conditions, and the last two terms in (10) reflect the presence of the external field. This external field is associated to strongly non-linear contributions in $K(t)$ that prevents us from using a standard Laplace transformation [31] to solve equation (10). To deal with these non-linearities we propose an appropriate ansatz for the long time behavior of $K(t)$ and then, keeping consistency, follow usual techniques for solving differential equations. We introduce the ansatz:

$$\int_0^t K^{1/2}(t')e^{-A(0)(t-t')}dt' = \zeta K^{1/2}(t) \quad (13)$$

and solve for $K(t)$, determining ζ self-consistently. With this ansatz, the problem has been reduced to find a solution for a linear differential equation in $K(t)$, a function that encloses conditions (4), (8) and (9). Once $K(t)$ is known, observables like response functions, two times autocorrelations, and spatial correlation functions can be readily obtained. Spatial correlations are given by:

$$\begin{aligned}C(\mathbf{x}, \mathbf{x}', t, t) &= C(R, t) = \int \frac{d^dk}{(2\pi)^d} \\ &\times\int \frac{d^dk'}{(2\pi)^d} e^{i(\mathbf{k}\cdot\mathbf{x} + \mathbf{k}'\cdot\mathbf{x}')} \langle\hat{\phi}(\mathbf{k}, t)\hat{\phi}(\mathbf{k}', t)\rangle\end{aligned}\quad (14)$$

where $R = |\mathbf{x} - \mathbf{x}'|$, while two-times autocorrelations are defined as:

$$\begin{aligned}C(\mathbf{x}, \mathbf{x}, t, t') &= C(t, t') = \int \frac{d^dk}{(2\pi)^d} \\ &\times\int \frac{d^dk'}{(2\pi)^d} e^{i(\mathbf{k} + \mathbf{k}')\cdot\mathbf{x}} \langle\hat{\phi}(\mathbf{k}, t)\hat{\phi}(\mathbf{k}', t')\rangle.\end{aligned}\quad (15)$$

Table 1. Long time solutions for $C(t, t')$ and $C(R, t)$ at $T = 0$ for different values of the applied field in ZFC case.

h	$C(t, t')$	$C(R, t)$
$h < h_c$	$C_\infty + \frac{(tt')^{\frac{1}{4}}}{(t+t')^{\frac{1}{2}}}$	$f(R) + C_\infty$
$h = h_c$	$C_\infty + \frac{1}{(tt')^{\frac{1}{4}}(t+t')^{\frac{1}{2}}}$	$f(R)/t + C_\infty$
$h > h_c$	$C_\infty + \frac{e^{-\frac{1}{2}\lambda(t+t')}}{(t+t')^{\frac{1}{2}}}$	$f(R)e^{-\lambda t}/\sqrt{t} + C_\infty$

Below we present and discuss the analytical predictions for some of these observables and leave to Appendix A the details of the calculations.

2.1 Observables at $T = 0$

At zero temperature and in both the disordered (zero field cooled) and ferromagnetic (field cooled) quenches, we have found a critical field which divides the analysis in three regions $h < h_c$, $h = h_c$ and $h > h_c$, with qualitatively different long time dynamics (the critical field is defined in Appendix A). Starting from the ferromagnetic configuration we show that, despite the existence of this critical field, the decay of the correlation functions are essentially exponential, although with different exponential or constant rates. However, if the quench is done starting from a disordered high temperature phase, we find important functionality changes in the two-time and the spatial correlation functions as a function of h .

2.1.1 Zero field cooling

In Table 1 we show the predicted long time behavior of the spatial and two-times autocorrelation functions in ZFC experiments.

C_∞ is a constant which is different in each expression and

$$f(R) = \frac{1}{(k_0 R)^{\frac{d}{2}-1}} J_{\frac{d}{2}-1}(k_0 R) e^{-\frac{R^2}{4A_2 t}}, \quad (16)$$

where $J_n(x)$ is a Bessel function of the first kind.

As can be seen, for $h \leq h_c$ autocorrelations show aging behavior. In particular, the asymptotic ($t \gg t'$) two-times correlation function has the form $C(t, t') \propto (L(t)/L(t'))^\nu$ that characterizes a coarsening dynamics caused by the competition of domains of modulated structures [31]. The typical size of these domains grows as $L(t) \propto t^{1/2}$, as can be confirmed from the exponential term of $f(R)$ in the $h < h_c$ spatial correlations. On the other hand, for $h > h_c$ the autocorrelations relax exponentially fast to the asymptotic value. Also, it is worth to note the independence of the two-times autocorrelations with the dimensionality of the system.

The spatial correlations at zero temperature show that only for $h < h_c$ the system establishes modulated structures at infinite time.

Table 2. Long time solutions for $C(R, t, t')$ and $C(R, t)$ at zero temperature for FC protocols.

h	r_0	$C(R, t, t')$
$h = 0$	$r_0 > -A(0)$	$C_\infty e^{-(r_0 + A(0))(t+t')}$
$h = 0$	$r_0 < -A(0)$	$C_\infty + e^{2(r_0 + A(0))t}$
$h > 0$		$C_\infty + e^{-\frac{1}{2}(\lambda + A(0))(t+t')}$

2.1.2 Field cooling

Because the initial condition is homogeneous ($\phi(\mathbf{x})$ is constant), the correlations in this case are independent of R .

As already mentioned, in this case $K(t)$ is essentially exponential for any value of h (see Appendix A.1 for more details). Moreover, the dominant exponential terms depend strongly on h . In particular, for $h = 0$ one finds that the form of $C(t, t')$ depends on the ratio between r_0 and $A(0)$, as it is shown in Table 2.

The fact that auto-correlations decay to zero or non-zero constants according to the values of r_0 and $A(0)$ can be understood in terms of the stability of the component $\hat{\phi}(k = 0)$. For $r_0 > -A(0)$ the $k = 0$ mode is stable and the system evolves to a non-magnetized state. When $r_0 < -A(0)$ the instability of the zero mode drives the system to a non-zero magnetization.

For $h > 0$, the decay rate depends on a parameter λ that encloses the dependency on h (see Eq. (A.19)). The point $\lambda(h_c) = 0$ defines the critical field. Above this value of h the decay rate depends only on $A(0)$ and measures, essentially, how fast the system relaxes to the asymptotic ferromagnetic state.

3 Numerical simulations

With the aim to test the predictions of the Hartree approximation we solved numerically the dynamical equations (3) for the particular case of a two dimensional model of magnetic film with competing exchange and dipolar interactions in the limit of strong perpendicular anisotropy, in which case the interactions are perfectly isotropic [35]. The continuum nature of the model and the isotropy of interactions pose some serious challenges to the accuracy and interpretation of numerical solutions. We devote this section to discuss our strategy in order to obtain meaningful results. We start the section with a discussion of the spectrum of fluctuations of the model, how it is affected by finite size and discretization of space and time, that are inevitable when solving differential equations numerically, and propose some strategies to minimize these effects. After that, we describe the actual numerical scheme used to solve the equations. Finally, the numerical results are discussed and compared with the analytic ones from previous sections.

3.1 The spectrum of fluctuations

We discretize the system in a square mesh of $L \times L$ sites. In the discretized reciprocal space, the function $f(t)$ defined

in (12) for the continuum system takes the form:

$$f(t) = \frac{1}{L^2} \sum_{\mathbf{k}} e^{-2A(\mathbf{k})t}, \quad (17)$$

where

$$\mathbf{k} = \left(\frac{2\pi}{aL} i, \frac{2\pi}{aL} j \right) \quad i, j = -\frac{L}{2} + 1, \dots, \frac{L}{2}, \quad (18)$$

a is the linear size of the mesh and $A(\mathbf{k})$ is given by (7). From (17) we should note that only for $L \gg 1$ and a sufficiently small value of the mesh a the discrete version of $f(t)$ can be approximated by the continuum one.

At this point it is worth to note that, even in the continuum formulation, the functionality $f(t) \sim 1/t^{1/2}$ is only valid for $t \gg \tau_c$, in which the function under the integral (12) is sharp enough (see Appendix A and [31]). Moreover, for sufficiently long times, the discrete nature of $A(\mathbf{k})$ provokes deviations of $f(t)$ from the expected power law behavior. The characteristic time in which this deviation happens should be of the order of the inverse of the difference between $A(\mathbf{k}_0)$ and $A(\mathbf{k})$, with \mathbf{k} a nearest neighbor vector of \mathbf{k}_0 .

Up to now we have not specified the nature of the competing interaction $J(\mathbf{x}, \mathbf{x}')$ in (1). In ultrathin ferromagnetic films with strong perpendicular anisotropy, the competing interactions are the short range exchange (represented in the continuum model by the square gradient term in (1)) and the long ranged dipolar interaction. In the limit of strong perpendicular anisotropy, the dipolar moments point (except at domain walls) out of the plane of the sample, and the magnetization can be modeled by a continuum scalar field $\phi(\mathbf{x})$. In this limit the dipolar term takes the form $J(\mathbf{x}, \mathbf{x}') \propto 1/|\mathbf{x} - \mathbf{x}'|^3$. Note that in this limit the interactions are perfectly isotropic and so will be the spectrum of Gaussian fluctuations. The long range nature of dipolar interactions is commonly taken into account by means of the so-called Ewald summation technique [36]. Unfortunately, the use of the $\hat{J}(k)$ given by the Ewald sums provokes a growing anisotropy in the fluctuation spectrum as the wave vector \mathbf{k} approaches the value π/a . This makes the minima of the fluctuation spectrum to remain in a finite number of directions. In this way, after certain time, the parabolic nature of the isolated minima provokes a crossover in the exponent of the power law in $f(t)$ from $-1/2$ to a dimensional dependent value $-d/2$, as it is shown in Figure 1 for $d = 2$. This new exponent coincides with the one obtained for the purely ferromagnetic system [32,37], where $f(t)$ is dominated by the single minimum of the fluctuation spectrum at $\mathbf{k} = 0$.

In general, this long time behavior must appear in any system characterized by several isolated minima in the fluctuation spectrum. In this sense, it is important to be aware of this subtle anisotropic effect introduced by the Ewald technique.

In order to avoid these undesired effects, a possibility is to replace $\hat{J}(k)$ by its expansion for small k up to second order, as has been already made in literature [38]. However, a more justified approach in the context of magnetic thin films is to consider the two-dimensional Fourier

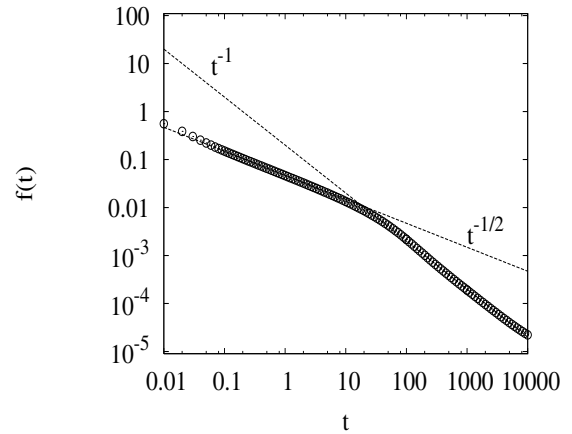


Fig. 1. Behavior of $f(t)$ for dipolar frustrated ferromagnetic model of size $L = 1200$, using the $\hat{J}(k)$ given by the Ewald sums. For sufficiently large sizes a crossover is observed in the power law exponent from $-1/2$ to -1 .

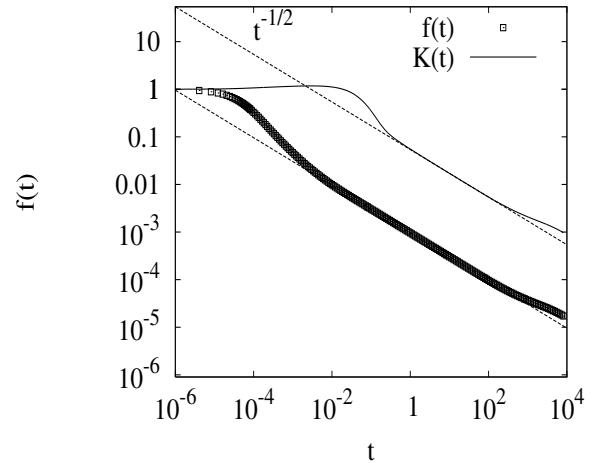


Fig. 2. Behavior of $f(t)$ for a system of $L = 1960$ using the $\hat{J}(k)$ given by expression (19). The behavior of $K(t)$ for $h = 0$ is also shown. The deviation from power law for large times is a finite size effect.

transform of the kernel of the actual dipolar interaction $1/r^3$. That is

$$\hat{J}(k) = -2\pi k + \frac{2\pi}{\alpha} F \left[-\frac{1}{2}, \left(\frac{1}{2}, 1 \right), -\frac{1}{4}k^2\alpha^2 \right] \quad (19)$$

where F is the confluent hypergeometric function and α is a short distance cutoff.

Figure 2 shows the behaviors of $f(t)$ and $K(t)$ using the $\hat{J}(k)$ given by (19). The range of times in which $f(t)$ follows a power law with the predicted exponent is determined only by τ_c and an upper bound dependent on the size of the system.

3.2 Numerical scheme

In order to build a numerical scheme it is useful to express (3) in a dimensionless form. A natural choice for the

characteristic length is the wave length corresponding to the minimum of the spectrum of fluctuations $\lambda_0 = 2\pi/k_0$. Taking $J(\mathbf{x}, \mathbf{x}')$ as the dipolar interaction with a short distance cut-off α described in the last subsection, this characteristic length is given by $\lambda_0 = 2\delta(1 + \pi\alpha/2\delta)$. Defining also a characteristic time $t_0 = \lambda_0^2/\Gamma$ and a characteristic field value $\phi_s = \sqrt{r/u}$, we can define new reduced variables as

$$\frac{\mathbf{x}}{\lambda_0} \rightarrow \mathbf{x}, \quad \frac{t}{t_0} \rightarrow t, \quad \frac{\delta}{\lambda_0} \rightarrow \delta, \quad \frac{\alpha}{\lambda_0} \rightarrow \alpha, \quad \frac{\phi}{\phi_s} \rightarrow \phi. \quad (20)$$

Equation (3) can be rewritten as:

$$\frac{\partial \phi(\mathbf{x}, t)}{\partial t} = \nabla^2 \phi(\mathbf{x}, t) - \frac{1}{\delta} \int d^2 \mathbf{x}' J(|\mathbf{x} - \mathbf{x}'|, \alpha) \phi(\mathbf{x}', t) + \beta[\phi(\mathbf{x}, t) - \phi^3(\mathbf{x}, t)] + h + \sqrt{2T} \eta(\mathbf{x}, t) \quad (21)$$

where we have defined the dimensionless variables

$$\frac{h\lambda_0^2}{\phi_s^2} \rightarrow h, \quad \lambda_0^2 r \rightarrow \beta, \quad \frac{T}{\phi_s^2} \rightarrow T, \quad (22)$$

and the thermal noise has been normalized in such a way that $\langle \eta(\mathbf{x}, t) \eta(\mathbf{x}', t') \rangle = \delta(t - t') \delta(\mathbf{x} - \mathbf{x}')$. So, we can write in the reciprocal space

$$\frac{\partial \hat{\phi}(\mathbf{k}, t)}{\partial t} = - \left[k^2 + \frac{1}{\delta} \hat{J}(k) - \beta \right] \hat{\phi}(\mathbf{k}, t) + \left[h - \beta \phi^3(\mathbf{x}, t) + \sqrt{2T} \eta(\mathbf{x}, t) \right]_{\mathbf{k}}^F \quad (23)$$

where $\int_{\mathbf{k}}^F$ means the \mathbf{k} component of the corresponding Fourier transform.

We discretize the space with a mesh size $a = 1/M$. Since λ_0 is our characteristic length, this implies that the wave-length of the modulated structures consists in approximately M sites of the simulation system. Now, if we want the system to be able to show N modulated structures, we must simulate a square lattice with a linear size of $L = MN$ sites. Thus, we construct a scheme in which M and N are fixed at a large enough value to ensure realistic simulations for the continuum model. In this sense, both quantities play a well-defined role. Increasing M is associated with an improvement of the domain wall dynamics as the magnetic structures can extend over several mesh sites. This results in a better definition of the time τ_c in which $f(t)$ reaches its long times behavior. On the other hand, increasing N allows us to see a larger fraction of the (ideally infinite) system and is related to the growth of the maximum time for which $f(t)$ can still be approximated to its long time functionality.

In order to further simplify the spatially discretized dimensionless equation we now repeat the transformations in equation (20) for both space and time variables using a in place of the characteristic length ($\mathbf{k}a \rightarrow \mathbf{k}$ and $t/a^2 \rightarrow t$), and redefine the strength of the local potential as $a^2\beta \rightarrow \beta$. Finally we consider a standard first-order semi-implicit spectral integration scheme, with a time step

dt , to construct the following recurrence relation:

$$\hat{\phi}(\mathbf{k}, t + dt) = \frac{\hat{\phi}(\mathbf{k}, t)}{1 + k^2 dt} \left[1 + dt(\beta - a\hat{J}(\mathbf{k})/\delta) \right] + \frac{dt \left[-\beta \phi^3(\mathbf{x}, t) + a^2 h + \sqrt{\frac{2T}{dt}} \eta(\mathbf{x}, t) \right]_{\mathbf{k}}^F}{1 + k^2 dt}$$

where the noise term η is a random Gaussian number with unit variance. Here we are taking advantage of the isotropic form of the laplacian in the inverse space, where the adimensional wave vector has the form $\mathbf{k} = (2\pi i/L, 2\pi j/L)$.

3.2.1 Choosing simulation parameters

Simulations were carried out for a system of $M = 35$ and $N = 56$, that is $L = 1960$, with the parameters $\alpha = 0.04$, $\beta = 0.265$. From the chosen form of the dipolar interaction we have δ fixed as $\delta = (1 - \pi\alpha)/2$. The value of M was chosen to be large enough as to guaranty the convergence of τ_c to the continuum system value. To have a good estimate of the simulation time needed to reach the asymptotic regime of the model, we first solved numerically equation (10) (see Fig. 2). One can see that the time at which the asymptotic functionality of $K(t)$ sets in has a lower bound different from that of $f(t)$, this bound is dependent on the whole set of parameters and is greater than τ_c .

Comparing our numerical scheme with equation (3) it is possible to express the parameters r_0 , $A(0)$ and g used in analytical calculations as

$$\begin{aligned} r_0 &= \mathcal{A}(k_0) \\ A(0) &= \mathcal{A}(0) - \mathcal{A}(k_0) \\ g &= 3\beta \end{aligned} \quad (24)$$

where $\mathcal{A}(k)$ is the numerical fluctuation spectrum. In this way the critical field can be written as

$$h_c = \frac{1}{a^2} \sqrt{\frac{-\mathcal{A}(k_0)}{3\beta}} [\mathcal{A}(0) - \mathcal{A}(k_0)] \quad (25)$$

that, under our particular set of parameters takes the value $h_c = 4.53$.

3.3 Simulation results

In our simulations, the system is initialized in a disordered (homogeneous) configuration corresponding to the ZFC (FC) experiment. Suddenly, a subcritical temperature is fixed and the system is let to evolve a time t_w , simulating a quench. Then, autocorrelations are computed as function of the time Δt elapsed after t_w .

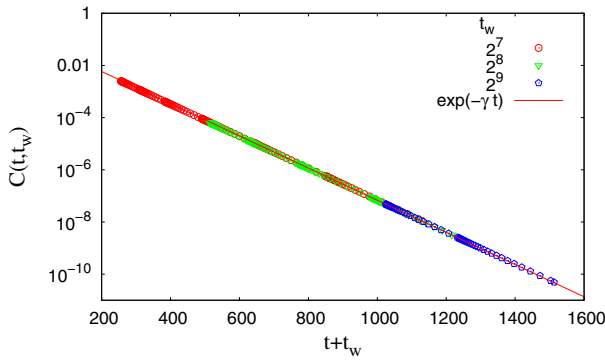


Fig. 3. (Color online) Self-correlations for $r_0 > -A(0)$ in the $T = 0$ and $h = 0$ ferromagnetic quench.

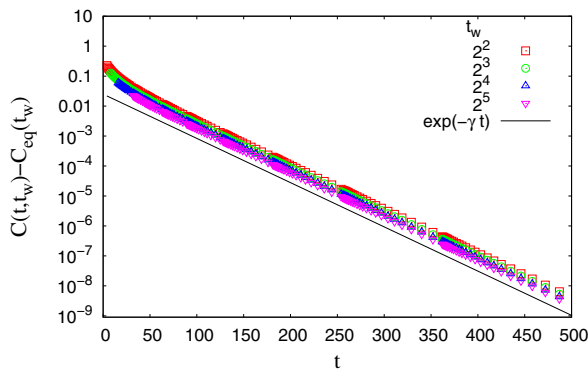


Fig. 4. (Color online) Self-correlations for $r_0 < -A(0)$ in the $T = 0$ and $h = 0$ ferromagnetic quench.

3.3.1 Field cooling

We present first, the dynamical behavior of the system after a quench from a fully magnetized state for $T = 0$ and $h < h_c$. In particular, we focus our attention of the differences between the cases $r_0 > -A(0)$ and $r_0 < -A(0)$ at $h = 0$ (see Tab. 2). Tuning the value of β , and starting from the same initial conditions, one can study both cases.

In Figures 3 and 4 we show autocorrelations for $r_0 > -A(0)$ and $r_0 < -A(0)$ respectively. In both cases, the numerical estimations fit very well with the asymptotic predictions in Table 2. In addition also the exponential factors characterizing the decay rates ($r_o + A(0)$) of these correlations are consistent with the analytical predictions. The difference between the theoretical values for the parameters used and the numerical estimation obtained fitting the numerical data is smaller than 5 percent.

At zero temperature, as we already mentioned, a system evolving from homogeneous ferromagnetic initial conditions is incapable to break the spatial homogeneity. In this context, the fact that autocorrelations decay to zero or non-zero constants according to the values of r_0 and $A(0)$ can be understood in terms of the stability of the component $\hat{\phi}(k = 0)$. For $r_0 > -A(0)$ one has from (24) that $A(0) > 0$. This in turn implies that the $k = 0$ mode is unstable and the system evolves to a non-magnetized state.

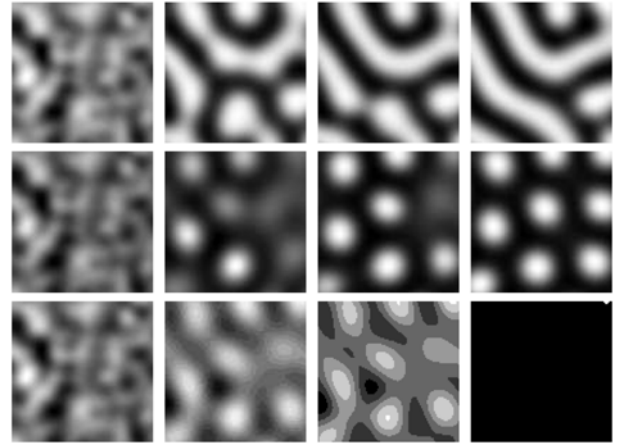


Fig. 5. Evolution of the magnetization patterns of a 100×100 portion of the 1960×1960 system for three different fields after a disordered quench. First row: $h = 0$, second row: $h = 4.0 < h_c$ and third row: $h = 4.7 > h_c$. Time grows from left to right.

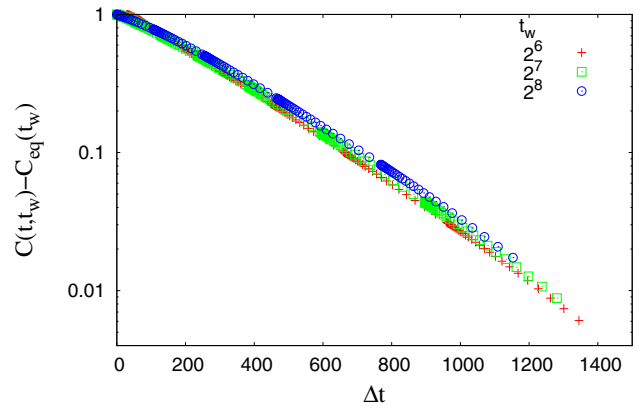


Fig. 6. (Color online) Autocorrelations in the ZFC case for $T = 0$ and $h > h_c$ and several waiting times. An asymptotic exponential relaxation is observed in agreement with analytic results in Table 1.

On the contrary, for $r_0 < -A(0)$ the stability condition $A(0) < 0$ drives the system to a non-zero magnetization.

3.3.2 Zero field cooling

The effects of the predicted critical field (A.10) can be seen in Figure 5.

There, three dynamical sequences are shown after a disordered quench for field values above and below the critical one. It can be seen that final configurations evolve, correspondingly, to modulated or homogeneous states as expected from our results (see Tab. 1) and also predicted by thermodynamic equilibrium studies [35].

Autocorrelations for $T = 0$ and $h > h_c$ decay very rapidly to a plateau which is dependent on t_w . In Figure 6 the quantity $C_{eq}(t_w)$ has been subtracted. It is seen that, as time grows, the exponential decays become evident, in agreement with analytical results in Table 1.

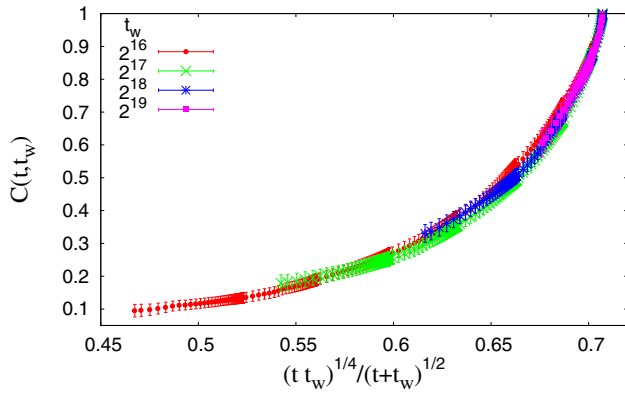


Fig. 7. (Color online) Collapse of the autocorrelations for the ZFC case, at $T = 0$ and $h = 0$, using 12 samples.

For $h = 0$, Figure 7 shows a reasonable agreement with the predicted collapse of the two-time autocorrelations (see Tab. 1 and [31]) in the asymptotic regime, attained for waiting times greater than 5×10^5 time steps.

Finally, an important result concerns the growth law of domains at low temperatures, as discussed in the introduction. Our analytical results of equation (16) predict $\xi_k(t) \simeq t^{1/2}$, where $\xi_k(t)$ is a positional correlation length. In Figure 8 we show the time dependence of the azimuthally averaged structure factor, the positional correlation length and the orientational correlation length, defined in [36]. At long times all quantities seem to follow a logarithmic growth, at variance with the power law with $z = 2$ found analytically. This slower regime may be due to pinning of topological defects, as observed in a similar model by Hou et al. [21] and Boyer et al. [26], as well as in a different model by Gomez et al. [29], which is not captured by the Hartree approximation.

In fact, the violation of scaling is common in low dimensional systems with topological textures, such as the two-dimensional XY model, where the growth law can also depend on whether or not the initial conditions contains unbounded vortices [39]. Numerical simulations of quenches from high temperatures to the ordered phase of this system have also pointed out that both topological (vortex) and nontopological (spin-wave) contributions are asymptotically relevant to the characteristic $L \sim (t/\ln(t))^{1/2}$ growth law [40]. Though a more careful work is needed to fully elucidate the origin of the logarithmic relaxation observed in Figure 8, we believe that both field fluctuations and defect pinning have important contributions to slow the system down.

4 Conclusions

We studied the Langevin dynamics of a model with competing isotropic interactions at different scales at $T = 0$ in the presence of an external field. Analytic results were

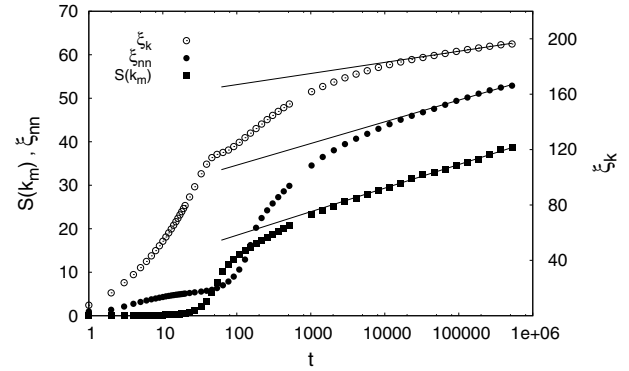


Fig. 8. Growing order in the disordered quench dynamics at $T = 0$ and $h = 0$ through the characteristic orientational and positional length scales ($\xi_{nm}(t)$ and $\xi_k(t)$), and the peak of the azimuthal average of the structure factor ($\hat{S}(k_m)$), shown in a log-linear scale. Error bars are smaller than point size and the solid lines corresponds to logarithmic fits and are guidelines for the eye only.

found in the self-consistent field (Hartree) approximation for two-time autocorrelation functions and also for spatial correlations. Two different dynamical protocols (initial conditions) were considered: zero field cooled and field cooled. Analytical results were confronted with numerical simulations of a prototypical system consisting of a ferromagnetic interaction frustrated with long range dipolar interactions in two dimensions. A detailed numerical scheme was developed and discussed.

Both analytically and numerically we found a critical field h_c which divides the long time dynamic behavior of the model in two regions: for $h \leq h_c$, the long time dynamics strongly depends on the particular initial condition, while for $h > h_c$ the initial conditions are irrelevant. The regime $h \leq h_c$ corresponds to the appearance of modulated structures at low temperatures (stripes or bubbles), while for $h > h_c$ the system is a paramagnet in an external field.

We obtained explicit expressions for the autocorrelations and spatial correlation functions, both for the disordered and ferromagnetic quenches, considering all possible values of temperature and external applied field. In the FC case relaxations are essentially exponential. In the ZFC case the system presents a slow coarsening of modulated domains. This coarsening process reflects in an aging behavior of the two-time correlation functions. The analytical prediction for the aging scaling is in reasonable agreement with the numerical results. The results for the spatial correlations predict a growth law for the modulated domains with a power law $\xi \simeq t^{1/2}$. This is not verified numerically, but a logarithmic growth $\xi \simeq \ln t$ at long times is observed instead. This slow logarithmic behavior may be consequence of the very slow drift of topological defects, which are not taken into account by the self-consistent field approximation.

Finally, it is important to remark that although the Hartree approximation does not consider the influence of topological defects in the dynamical behavior, our

numerical results at $T = 0$ compare quite well with the predictions of the theory. Surely topological defects are very important in the long time dynamics of the system and must be included in a complete theory of dynamics of modulated systems. Nevertheless, after a quench at zero temperature the dynamics of defects is extremely slow, such that our approximate theory can still give valuable information on the relaxation in a time scale where defects can be considered as effectively “quenched”.

We gratefully acknowledge partial financial support from the Abdus Salam ICTP through grant *Net-61, Latinamerican Network on Slow Dynamics in Complex Systems*. Calculation facilities kindly offered by the Bioinformatic’s Group of the Center of Molecular Immunology in Cuba were instrumental to this work. L. N. and D. A. S. would like to thank partial financial support from CNPq, Brazil.

Appendix A: Solution for $K(t)$ at $T = 0$

In this case equation (10) for $K(t)$ takes the form:

$$\begin{aligned} \frac{dK(t)}{dt} = & 2r_0K(t) + 2gV(t) \\ & + 4gh K(t)^{1/2}\phi_0 e^{-A(0)t} \\ & \times \int_0^t d\tau K(\tau)^{1/2} e^{-A(0)(t-\tau)} \\ & + 2gh^2 \left[\int_0^t d\tau K(\tau)^{1/2} e^{-A(0)(t-\tau)} \right]^2. \end{aligned} \quad (\text{A.1})$$

Here a hypothesis is done as a very important step of the calculation that will allow us to linearize equation (A.1), namely:

$$\begin{aligned} \int_0^t K^{1/2}(t') e^{-A(0)(t-t')} dt' = & \zeta K^{1/2}(t) \\ & A(0)t \gg 1, \end{aligned} \quad (\text{A.2})$$

and its consistency will be proved in the solution process, since the parameter ζ is determined self-consistently using the hypothesis itself. By means of (A.2), equation (A.1) reads

$$\begin{aligned} \frac{dK(t)}{dt} = & 2r_0K(t) + 2gV(t) + 4gh \phi_0 e^{-A(0)t} \\ & \times \zeta K(t) + 2gh^2 \zeta^2 K(t). \end{aligned} \quad (\text{A.3})$$

The term $4gh \phi_0 e^{-A(0)t} \zeta K(t)$ is unimportant in the long time limit, because it decays faster than others in the equation, given that $A(0) > 0$. Then, in the long time limit, we have to solve the following ordinary linear differential equation:

$$\frac{dK(t)}{dt} = (2r_0 + 2gh^2 \zeta^2)K(t) + 2gV(t). \quad (\text{A.4})$$

The general solution of this equation is

$$\begin{aligned} K(t) = & K(0)e^{(2r_0+2gh^2\zeta^2)t} \\ & + 2g \int_0^t d\tau V(\tau) e^{(2r_0+2gh^2\zeta^2)(t-\tau)}. \end{aligned} \quad (\text{A.5})$$

Different kind of solutions in the long time limit are possible according to the sign of $2r_0 + 2gh^2\zeta^2$.

If $2r_0 + 2gh^2\zeta^2 > 0$, then:

$$\begin{aligned} K(t) = & \left(K(0) + 2g \int_0^\infty d\tau V(\tau) e^{-(2r_0+2gh^2\zeta^2)\tau} \right) \\ & \times e^{(2r_0+2gh^2\zeta^2)t}. \end{aligned} \quad (\text{A.6})$$

The integral converges because $V(t)$ is a bounded, decreasing function of t . In this case we obtain a general solution independently of the particular function $V(t)$.

If $2r_0 + 2gh^2\zeta^2 = 0$:

$$K(t) = K(0) + 2g \int_0^\tau d\tau V(\tau). \quad (\text{A.7})$$

This solution is less general than the previous one. It is valid while the term given by the higher order correction to the hypothesis (A.2) is irrelevant in comparison with $V(t)$.

If $2r_0 + 2gh^2\zeta^2 < 0$, like before, there is not a general solution. The long time solution is given by the term decaying slower in expression (A.5).

It is possible to obtain a critical field as the lowest applied field h_c for which $K(t)$ is an exponential. To do this we suppose that $2r_0 + 2gh^2\zeta^2 > 0$. Then:

$$K(t) = C e^{(2r_0+2gh^2\zeta^2)t}, \quad (\text{A.8})$$

and with condition (A.2) we obtain the following equation for the parameter ζ :

$$\zeta = \frac{1}{r_0 + gh^2\zeta^2 + A(0)}. \quad (\text{A.9})$$

The limit case for which we have an exponential solution is when $2r_0 + 2gh_c^2\zeta^2 = 0$, applying this condition to the previous equation we get $\zeta_c = 1/A(0)$. Then, the critical field is given by:

$$h_c = \sqrt{-\frac{r_0}{g} A(0)}. \quad (\text{A.10})$$

This field defines a zone in the parameter space ($h > h_c$) in which the long time behavior of the system is universal, in the sense that it is independent of initial conditions.

A.1 $h \leq h_c$

We considered separately quenches from the disordered and ferromagnetic initial conditions.

A.1.1 ZFC, disordered case

With conditions (4) appropriately taken, the equation (A.1) for the ZFC system reads:

$$\begin{aligned} \frac{dK(t)}{dt} = & 2r_0K(t) + 2g\Delta f(t) \\ & + 2gh^2 \left[\int_0^t d\tau K(\tau)^{1/2} e^{-A(0)(t-\tau)} \right]^2 \end{aligned} \quad (\text{A.11})$$

where, in the long time limit, $f(t)$ is given by [31]:

$$f(t) = \alpha t^{-\frac{1}{2}}, \quad (\text{A.12})$$

$$\text{with } \alpha = \frac{k_0^{d-1}}{(2\pi)^d} \frac{2\pi^{\frac{d}{2}}}{\Gamma(\frac{d}{2})} \sqrt{\frac{\pi}{A_2}}.$$

We need to solve this equation considering the applied field to be lower than or equal to the critical one. In order to solve equation (A.11), we use hypothesis (A.2) obtaining the general solution:

$$K(t) = K(0)e^{(2r_0+2gh^2\zeta^2)t} + 2g\alpha\Delta \int_0^t \frac{d\tau}{\tau^{\frac{1}{2}}} e^{(2r_0+2gh^2\zeta^2)(t-\tau)}. \quad (\text{A.13})$$

Considering now $2r_0 + 2gh^2\zeta^2 < 0$ (that is $h < h_c$) we get, in the long time limit:

$$K(t) = \frac{-2g\alpha\Delta}{(2r_0 + 2gh^2\zeta^2)t^{\frac{1}{2}}}.$$

Applying condition (A.2) we obtain $\zeta = \frac{1}{A(0)}$, which allows us to rewrite $K(t)$ as:

$$K(t) = \frac{\alpha\Delta A^2(0)}{(h_c^2 - h^2)t^{\frac{1}{2}}}. \quad (\text{A.14})$$

When $h = h_c$, higher order corrections to the hypothesis (A.2) give:

$$K(t) = 4g\alpha\Delta \frac{A(0)}{A(0) - 2r_0} t^{\frac{1}{2}}. \quad (\text{A.15})$$

A.1.2 FC, ferromagnetic case

Using the initial conditions (4) equation (A.1) becomes:

$$\begin{aligned} \frac{dK(t)}{dt} &= 2r_0K(t) + 2g\phi_0^2 e^{-2A(0)t} \\ &+ 4gh\phi_0 e^{-A(0)t} \int_0^t d\tau K^{1/2}(\tau)e^{-A(0)(t-\tau)} \\ &+ 2gh^2 \left[\int_0^t d\tau K(\tau)^{1/2} e^{-A(0)(t-\tau)} \right]^2 \end{aligned} \quad (\text{A.16})$$

and, as before, using hypothesis (A.2) it is possible to arrive to the following general solution in the long time limit:

$$K(t) = K(0)e^{\lambda t} + 2g\phi_0^2 \int_0^t d\tau e^{-2A(0)\tau} e^{\lambda(t-\tau)}, \quad (\text{A.17})$$

where $\lambda = 2r_0 + 2gh^2\zeta^2$.

The analysis of the above solution when $h < h_c$ reveals different possibilities according to the different values of

the parameters involved. In the long time limit we obtain:
 $h = 0$

$$K(t) = \begin{cases} \left(1 + \frac{g\phi_0^2}{r_0+A(0)}\right) e^{2r_0t} & \text{for } r_0 > -A(0) \\ 2g\phi_0^2 t e^{-2A(0)t} & \text{for } r_0 = -A(0) \\ -\frac{g\phi_0^2}{r_0+A(0)} e^{-2A(0)t} & \text{for } r_0 < -A(0) \end{cases}$$

$h \neq 0$

$$K(t) = Ce^{\lambda t}. \quad (\text{A.18})$$

λ is given by the solution of the equation

$$\lambda = 2r_0 + \frac{2gh^2}{(A(0) + \frac{\lambda}{2})^2}, \quad (\text{A.19})$$

where hypothesis (A.2) has been used. Note that for all $h \leq h_c$ then $\lambda \leq 0$, being $\lambda(h_c) = 0$.

References

1. M. Seul, D. Andelman, *Science* **267**, 476 (1995)
2. O. Portmann, A. Vaterlaus, D. Pescia, *Nature* **422**, 701 (2003)
3. K. De'Bell, A.B. MacIsaac, J.P. Whitehead, *Rev. Mod. Phys.* **72**, 225 (2000)
4. J.M. Tanguada, B.J. Sternlieb, J.D. Axe, Y. Nakamura, S. Uchida, *Nature* **375**, 561 (1995)
5. S.A. Kivelson, E. Fradkin, V.J. Emery, *Nature* **393**, 550 (1999)
6. D.G. Barci, E. Fradkin, S.A. Kivelson, V. Oganesyan, *Phys. Rev. B* **65**, 245319 (2002)
7. G.H. Fredrickson, K. Binder, *J. Chem. Phys.* **91**, 7265 (1989)
8. G.H. Fredrickson, F.S. Bates, *Ann. Rev. Mater. Sci.* **26**, 501 (1996)
9. S.A. Brazovskii, *Sov. Phys. JEPT* **41**, 85 (1975)
10. C.L. Klix, C.P. Royall, H. Tanaka, *Phys. Rev. Lett.* **104**, 165702 (2010)
11. M. Tarzia, A. Coniglio, *Phys. Rev. Lett.* **96**, 075702 (2006)
12. H. Westfahl, J. Schmalian, P.G. Wolynes, *Phys. Rev. B* **64**, 174203 (2001)
13. M. Grousson, G. Tarjus, P. Viot, *Phys. Rev. E* **64**, 036109 (2001)
14. M. Grousson, V. Krakoviack, G. Tarjus, P. Viot, *Phys. Rev. E* **66**, 026126 (2002)
15. C. Roland, R.C. Desai, *Phys. Rev. B* **42**, 6658 (1990)
16. K.R. Elder, M. Grant, *J. Phys. A* **23**, L803 (1990)
17. J. Swift, P.C. Hohenberg, *Phys. Rev. A* **15**, 319 (1977)
18. P.C. Hohenberg, J.B. Swift, *Phys. Rev. E* **52**, 1828 (1995)
19. K.R. Elder, J. Viñals, M. Grant, *Phys. Rev. Lett.* **68**, 3024 (1992)
20. M.C. Cross, D.I. Meiron, *Phys. Rev. Lett.* **75**, 2152 (1995)
21. Q. Hou, S. Sasa, N. Goldenfeld, *Physica A: Statist. Mech. Appl.* **239**, 219 (1997)
22. J.J. Christensen, A.J. Bray, *Phys. Rev. E* **58**, 5364 (1998)
23. H. Qian, G.F. Mazenko, *Phys. Rev. E* **67**, 036102 (2003), and references therein
24. D. Boyer, J. Viñals, *Phys. Rev. E* **64**, 050101 (2001)

25. C. Sagui, R.C. Desai, Phys. Rev. E **49**, 2225 (1994)
26. D. Boyer, J. Viñals, Phys. Rev. E **65**, 046119 (2002)
27. C. Harrison, Z. Cheng, S. Sethuraman, D.A. Huse, P.M. Chaikin, D.A. Vega, J.M. Sebastian, R.A. Register, D.H. Adamson, Phys. Rev. E **66**, 011706 (2002)
28. C. Harrison, D.E. Angelescu, M. Trawick, Z. Cheng, D.A. Huse, P.M. Chaikin, D.A. Vega, J.M. Sebastian, R.A. Register, D.H. Adamson, Europhys. Lett. **67**, 800 (2004)
29. L.R. Gómez, E.M. Vallés, D.A. Vega, Phys. Rev. Lett. **97**, 188302 (2006)
30. P.M. Gleiser, F.A. Tamarit, S.A. Cannas, M.A. Montemurro, Phys. Rev. B **68**, 134401 (2003)
31. R. Mulet, D.A. Stariolo, Phys. Rev. B **75**, 064108 (2007)
32. T.J. Newman, A. Bray, J. Phys. A **23**, 4491 (1990)
33. F. Corberi, A. de Candia, E. Lippiello, M. Zannetti, Physica A **314**, 454461 (2002)
34. C. Chamon, L. Cugliandolo, H. Yoshino, J. Stat. Mech. (2006)
35. T. Garel, S. Doniach, Phys. Rev. B **26**, 325 (1982)
36. L. Nicolao, D.A. Stariolo, Phys. Rev. B **76**, 054453 (2007)
37. C. Godrèche, J.M. Luck, J. Phys.: Condens. Matter **14**, 1589 (2002)
38. E.A. Jagla, Phys. Rev. E **70**, 046204 (2004)
39. A.J. Bray, A.J. Briant, D.K. Jarvis, Phys. Rev. Lett. **84**, 1503 (2000)
40. F. Rojas, A.D. Rutenberg, Phys. Rev. E **60**, 212 (1999)